ChemPubSoc Europe

DOI: 10.1002/cssc.201501684

CHEMSUSCHEM Communications

Scalability of Continuous Flow Production of Metal–Organic Frameworks

Marta Rubio-Martinez,*[a] Trevor D. Hadley,[a] Michael P. Batten,[a] Keri Constanti-Carey,[a] Tim Barton,[a] Dylan Marley,[a] Andreas Mönch,[a] Kok-Seng Lim,[a] and Matthew R. Hill*[a, b]

Achieving the large-scale production of metal–organic frameworks (MOFs) is crucial for their utilization in applied settings. For many MOFs, quality suffers from large-scale, batch reaction systems. We have developed continuous processes for their production which showed promise owing to their versatility and the high quality of the products. Here, we report the successful upscaling of this concept by more than two orders of magnitude to deliver unprecedented production rates and space-time-yields (STYs) while maintaining the product quality. Encouragingly, no change in the reaction parameters, obtained at small scale, was required. The production of aluminium fumarate was achieved at an STY of 97159 kg m^{-3} day^{-1} and a rate of 5.6 kg h^{-1}.

Metal–organic frameworks (MOFs) are an emerging class of crystalline materials formed by the self-assembly of metal ions and organic components into a porous extended network.[1,2] In terms of combinations of metal nodes and organic linkers the number of networks that could be made is theoretically limitless. This offers many possibilities for the formation of new networks with novel architectures, which open paths to new advanced applications ranging from gas storage and separation[3] to drug delivery[4] or catalysis.[5] The ability to tune these materials to the specific requirements of an astonishing variety of uses is one of their fundamentally useful characteristics. However, after two decades of intense fundamental research on MOFs, the crucial prerequisite for accessing their potential applications, the ability to produce large quantities (kilogram-scale or higher) with high efficiency remains problematic.[6,7] To date, no synthetic approach fulfils these requirements, and of the thousands of known MOF structures only a few appear to be commercially available at the kilogram scale. We have only been able to identify 6 MOF structures, produced by BASF and distributed by Merck (Sigma–Aldrich): Basolite C300 (HKUST-1), A100 (MIL-53(Al)), Z1200 (ZIF-8), F300 (Fe-BTC), and Basosiv M050 (Mg-Formate), and UiO-66 distributed by STREM chemicals.[8]

Conventional MOF synthesis involves mixing solutions of the metal salt and organic linker in a sealed reactor vessel, which is subsequently heated for several hours under solvothermal conditions to promote the precipitation and growth of MOF crystals.[9,10] Recently, improvements of this approach have emerged, reducing the complexity and cost of the synthesis by operating at atmospheric pressures without the need for specialized equipment.[11,12] However, upscaling these solvothermal laboratory syntheses remains challenging due to long reaction times (hours or days), lack of versatility, and the low quality of materials ultimately obtained.[13,14]

Variations of solvothermal syntheses employ more efficient heating methods such as microwave or ultrasonic radiation, which accelerate the rate of chemical reaction and consequently reduce the reaction time from days to hours.[15] However, as MOF synthesis relies on the nucleation at a reactor vessel surface, the size of the vessel becomes a significant parameter. Reactions that proceed satisfactorily in small vessels may not always scale well to larger vessels at identical reaction conditions.[16,17] This limits the scaling of solvothermal methods to a smaller subset of MOFs that are more chemically robust in their preparation. To address these challenges, researchers have developed novel and radically different approaches, such as spray-drying and mechanochemical synthesis, as possible scale up techniques for MOF synthesis.[18,19] Despite the potential of these approaches a viable scale-up strategy remains to be found. To date none of these techniques, including semi-batch synthesis, have been scaled to continuous production of MOFs; a critical requirement for the production process to become economically viable. Switching from batch to continuous production removes cyclic processes such as preparation, heating, and cooling, and offers several benefits of continuous steady-state operation such as significantly reduced down-times, labour costs, reactor volumes, as well as constant and consistent production.[20,21]

Recently we described an optimised continuous-flow chemistry system for the production of a diverse range of MOFs, each with different reaction requirements. This demonstrated the versatility and reproducibility of continuous flow reaction conditions, which is crucial in MOF synthesis.[22,23] To the best of our knowledge, there is only one example showing the continuous large-scale hydrothermal production of ZIF-8, described by Lester and co-workers. Their setup uses a counter-current mixing reactor operating at 400 °C and 240 bar, yielding a production rate of 0.81 kg h^{-1}.[24]

[a] Dr. M. Rubio-Martinez, T. D. Hadley, Dr. M. P. Batten, K. Constanti-Carey, T. Barton, D. Marley, A. Mönch, Dr. K.-S. Lim, Dr. M. R. Hill
CSIRO
Private Bag 10, Clayton South VIC 3169 (Australia)
E-mail: marta.rubio@csiro.au
matthew.hill@csiro.au

[b] Dr. M. R. Hill
Department of Chemical Engineering
Monash University
Clayton VIC 3800 (Australia)

Supporting Information for this article can be found under http://dx.doi.org/10.1002/cssc.201501684.

Herein we study, for the first time, the scalability of continuous-flow chemistry production of MOFs, using a water-based synthesis of aluminium fumarate MOF (Al-Fum) as an example.[25] Our production is validated at 139 times the size of our laboratory system (from 10 mL to 1.394 L), enabling the production of 5.6 kg h^{-1}. Moreover, we translate the reaction parameters from milligram-scale to pilot-plant scale without any reoptimization of the reaction conditions (Figure 1).

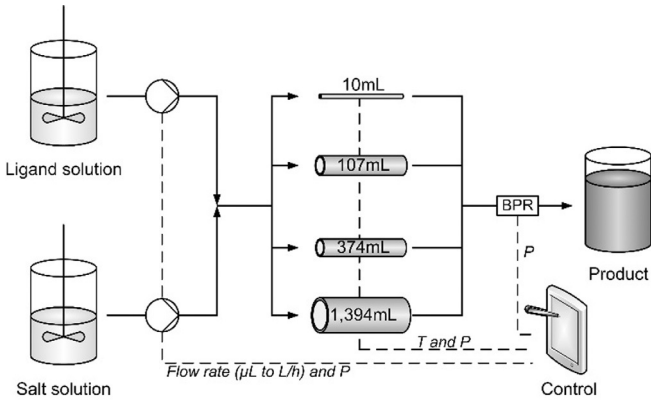

Figure 1. Schematic of the metal-organic framework scale-up production using flow chemistry. The precursor solutions are pumped continuously, mixed via a static-mixer into the 10, 107, 374 and 1394 mL reactors. On exiting the reactor zone, the stream is passed through a back-pressure regulator (BPR) and then collected into a collection flask.

Our scale-up strategy is based on maximizing the increase in reactor throughput associated with an increase in the tube number and/or diameter while managing a reduction in surface area to volume ratio (*SA/V*) of the reactor vessel. Minimizing changes in the *SA/V* ratio of the reactor vessel in each size stage is desirable to maintain the thermal and mass transport properties of the reactor.[26,27] The flow production rate of a given reactor can be increased by: (i) increasing the number of same-sized tubes in parallel, and (ii) increasing the diameter of those tubes. The volumetric flow rate (F_r) increases with the square of the tube diameter (d_t); that is, $F_r \propto d_t^2$. However, the *SA/V* ratio of the reactor tube decreases as tube diameter increases ($SA/V \propto 1/dt$, Figure 2). The degree of mixing in the reactor tube influences the reaction, with an increase in mixing favoring better mass and heat transfer to and from the reactor wall, and hence aiding access to the reactor surface for nucleation. This degree of mixing is directly related to the flow dynamics in the tube, which is described by the dimensionless Reynolds Number (*Re*).[28] Because the tube sizes in microreactors restrict mixing to the laminar-flow type ($Re < 2100$), in the absence of static mixers and other flow mechanisms mixing is achieved solely by molecular diffusion.[29] However, turbulent flow ($Re > 4000$) results in a significant (orders of magnitude) increase in the diffusion over molecular diffusion and the increase is determined by the degree of turbulence.[30,31] Therefore the anticipated drop in available surface area for nucleation as well as for efficient heat transport, as a result of increasing the tube diameter, is attenuated by an associated increase

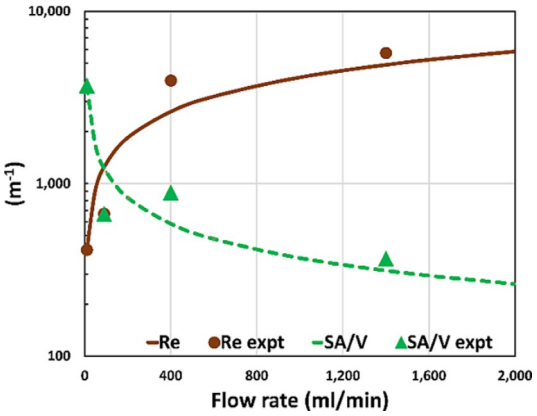

Figure 2. Impact of flow rate on Reynolds Number (*Re*) and surface area to volume ratio (*SA/V*) (m^{-1}), showing experimental results (symbols) and theoretical values (lines).

in the flow dynamics and mixing when moving from laminar to turbulent regime (see Figure 2). Over the scales investigated here the increased mixing due to turbulence has been sufficient to overcome the reduction in *SA/V* ratio (as witnessed by the product quality, and yield). However, it is most likely that further scale-up would require switching from increasing the diameter to increasing the number of scaled tubes.[28]

We performed the scale-up of MOF production using four different stainless-steel tubular flow reactors: a 10 mL coil tubing with $d_t = 1$ mm at laboratory scale, two intermediate stages with 107 mL ($d_t = 6$ mm) and 374 mL ($d_t = 4.5$ mm) reactor volume, and a pilot-scale 1.394 L reactor ($d_t = 10.9$ mm). In all four reactors, the precursor solutions were held separately and pumped into the reactors through a (T-type or Y-type) connector, where the two solutions were mixed. The reactants passed through the reactor with a controlled residence time, at a constant temperature. A back-pressure regulator was placed after the reactor coil to regulate the pressure and provide a uniform flow.

We chose Al-Fum MOF as a model system to demonstrate the scalability of our continuous-flow process. This microporous material exhibits high thermal stability up to 450 °C and presents a reversible uptake/release of water; in addition, it is a low-cost and low-toxicity MOF, making it suitable for many industrial applications, for example, in gas storage or heat exchangers.[32,33]

To start the synthesis process, we pumped separate precursor solutions of the organic ligand and the aluminium salt simultaneously through a static mixer into the heated tubular flow reactor at 65 °C using a residence time of 1 min. We used exactly the same precursor concentrations, reaction temperatures, and residence times for all four reactors (10, 107, 374 and 1394 mL). These parameters were determined through process optimisation, focusing on the highest production rate with the best MOF quality (for details on the optimisation process and flow equipment, see Table S1 and Figure S1 in the Supporting Information).

To evaluate the impact of our scaled flow approach we determined the quality of the produced material by Brunauer–

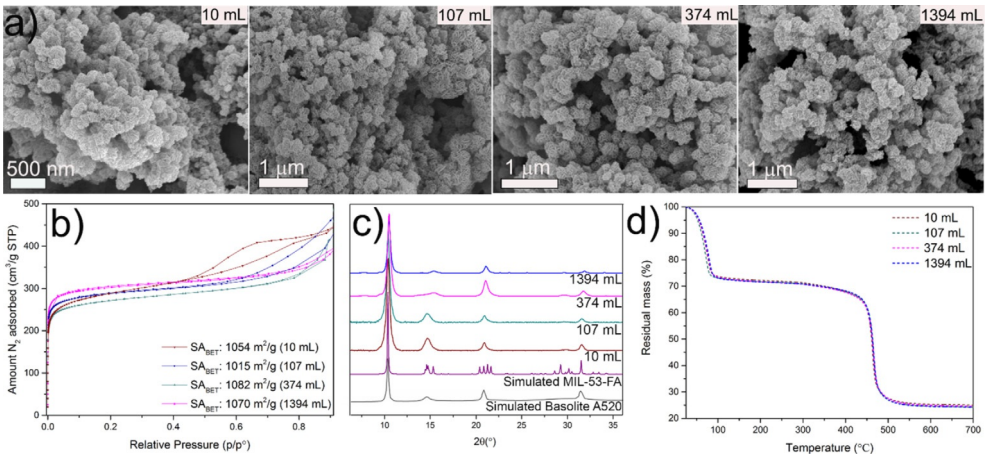

Figure 3. a) SEM image b) Experimental N_2 isotherm c) XRPD patterns and d) Thermogravimetric analysis using a heating rate: 5 °C min^{-1}) of the Al-Fumarate crystals synthesized by flow chemistry using the four different flow reactors.

Emmett–Teller (BET) surface area measurements, X-ray powder diffraction (XRPD), thermogravimetric analysis (TGA), and scanning electron microscopy (SEM), and compared the hourly rate of production. The diffraction patterns shown in Figure 3c confirm that the purity of the crystals obtained by flow chemistry in all cases is identical to the crystals synthesized by conventional solvothermal methods. The size and morphology of the crystals was established by SEM, as shown in Figure 3a. Standard N_2 adsorption measurements proved the porous character of the MOFs and yielded BET surface areas similar to values obtained by conventional methods (see Table S2). Some mesoporosity was witnessed in the Al-Fum synthesized with the microreactor due to interparticle packing between the nanometer-size crystallites as a consequence of a laminar flow, which leads a diffusion intermixing.

One way to measure process escalation is through the space–time-yield (STY) process parameter. This term, commonly used in catalytic reactor engineering, is defined as the amount of product produced per quantity of catalyst per unit time.[26] Here this refers to the amount of MOF produced (kg) per unit volume of reaction mixture (m^3) per day of synthesis.The larger the STY, the more economically viable the synthesis and thus, in order to increase the STY in a given MOF reaction, the amount of MOF produced per unit volume has to be maximized and the reaction time minimized (see Figure S2). To maximize the STY in the synthesis of Al-Fum we used the highest concentration of precursor solutions achievable at room temperature under normal stirring (0.35 M for the metal salt and 0.7 M of organic ligand) and a reaction time of 1 min. Table 1 and Figure 4 show the results of our attempts to maximize the STY.

In conclusion, we demonstrate the scalability of our continuous-flow chemistry approach to the synthesis of metal–organic frameworks (MOFs). An increase in scale of more than two orders of magnitude, high product quality, and an unprecedented space–time-yield (STY) were achieved. Our reactor design allows to translate reaction parameters from the laboratory scale to pilot scale without any reoptimization of the synthesis, while maintaining the STY values within the same range. In addition, the ability to produce a large variety of different MOFs, with high mass and energy transport efficiency, as well as precise control over the product's properties make this technology a game-changer for MOFs. Continuous-flow processing allows cost-efficient, large-scale production of these materials, thus bringing the many potential applications of MOFs closer to commercial reality.

Table 1. Production characteristics for different reactor volumes (Vol) and internal diameters (ID): flow rate, residence time (RT), production rate (PR), space–time yield (STY), and surface area (SA_{BET}).

Vol [mL]	ID [mm]	Flow rate [mL min^{-1}]	RT [min]	PR [g h^{-1}]	STY [kg m^{-3} d^{-1}]	SA_{BET} [m^2 g^{-1}]
10	1.0	10	1.0	33.8	81120	1070
107	6.0	90	1.2	325.5	73009	1015
374	4.5	400	0.9	1172.6	75247	1082
1394	10.9	1400	1.0	5643.3	97159	1054

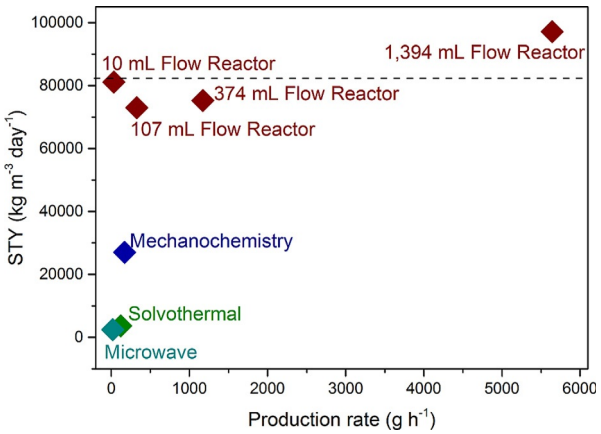

Figure 4. Production rate (g h^{-1}) vs. the space time yield (STY) for different synthetic pathways of Al-Fum.

Experimental Section

Synthesis of aluminium fumarate using a continuous flow reactor: An aqueous solution of 0.35 M $Al_2(SO_4)_3 \cdot 18H_2O$ and an aqueous solution of 0.7 M of fumaric acid and 2 M of NaOH solution were mixed under continuous flow conditions and heated in the different tubular reactors (10, 107, 374, and 1394 mL). The synthesis was conducted at 65 °C using a total flow rate of 10 mL min^{-1}, 90 mL min^{-1}, 374 mL min^{-1}, and 1394 mL min^{-1} giving a total residence time of ca. 1 min. The material was washed three times with fresh water and twice with ethanol and dried in vacuum for 8 h at 80 °C. The particle size is 216 ± 53 nm (10 mL), 274 ± 71 nm (107 mL), 267 ± 41 nm (374 mL), 284 ± 47 nm (1394 mL).

Characterization: The scanning electron microscopy (SEM) images were collected on a Quanta 400 FEG ESEM (FEI) at acceleration voltage of 0.2–30 kV. XRPD measurements were performed with an X'Pert Pro MPD diffractometer (Panalytical) over a 2θ range of 5°–45°. Gas adsorption isotherms for pressures in the range 0–120 kPa were measured by a volumetric approach using a Micrometrics ASAP 2420 instrument. All the samples were transferred to predried and weighed analysis tubes and sealed with Transcal stoppers. Al-fumarate samples were evacuated and activated under dynamic vacuum at 10^{-6} Torr at 140 °C for 8 h. Ultra-high purity N_2 was used for the experiments. N_2 adsorption and desorption measurements were conducted at 77 K. Surface area measurements were performed on N_2 isotherms at 77 K using the Brunauer-Emmer-Teller (BET) model with adsorption values increasing range of 0.005 to 0.2 relative.

Acknowledgements

The authors thank the CSIRO Engineering Workshop for the support in the construction of the flow reactor.

Keywords: aluminum fumarate · flow chemistry · metal-organic frameworks · rheology · synthetic methods

[1] J. R. Long, O. M. Yaghi, *Chem. Soc. Rev.* **2009**, *38*, 1213 – 1214.
[2] H.-C. "Joe" Zhou, S. Kitagawa, *Chem. Soc. Rev.* **2014**, *43*, 5415 – 5418.
[3] H.-C. Zhou, J. R. Long, O. M. Yaghi, *Chem. Rev.* **2012**, *112*, 673 – 674.
[4] P. Horcajada, R. Gref, T. Baati, P. K. Allan, G. Maurin, P. Couvreur, G. Férey, R. E. Morris, C. Serre, *Chem. Rev.* **2012**, *112*, 1232 – 1268.
[5] J. Lee, O. K. Farha, J. Roberts, K. A. Scheidt, S. T. Nguyen, J. T. Hupp, *Chem. Soc. Rev.* **2009**, *38*, 1450 – 1459.
[6] S. T. Meek, J. A. Greathouse, M. D. Allendorf, *Adv. Mater.* **2011**, *23*, 249 – 267.
[7] A. U. Czaja, N. Trukhan, U. Müller, *Chem. Soc. Rev.* **2009**, *38*, 1284.
[8] Materials Science Products," can be found under http://www.sigmaaldrich.com/materials-science/material-science-products.html?TablePage = 103996366, **n.d.**.
[9] G. Férey, *Chem. Soc. Rev.* **2008**, *37*, 191 – 214.
[10] S. Qiu, G. Zhu, *Coord. Chem. Rev.* **2009**, *253*, 2891 – 2911.
[11] C. McKinstry, R. J. Cathcart, E. J. Cussen, A. J. Fletcher, S. V. Patwardhan, J. Sefcik, *Chem. Eng. J.* **2016**, *285*, 718 – 725.
[12] D. Cattaneo, S. J. Warrender, M. J. Duncan, R. Castledine, N. Parkinson, I. Haley, R. E. Morris, *Dalton Trans.* **2016**, *45*, 618 – 629.
[13] D. Farrusseng, S. Aguado, C. Pinel, *Angew. Chem. Int. Ed.* **2009**, *48*, 7502 – 7513; *Angew. Chem.* **2009**, *121*, 7638 – 7649.
[14] P. Silva, S. M. F. Vilela, J. P. C. Tomé, F. A. Almeida Paz, *Chem. Soc. Rev.* **2015**, *44*, 6774 – 6803.
[15] N. A. Khan, S. H. Jhung, *Coord. Chem. Rev.* **2015**, *285*, 11 – 23.
[16] R. Ameloot, E. Gobechiya, H. Uji-i, J. A. Martens, J. Hofkens, L. Alaerts, B. F. Sels, D. E. De Vos, *Adv. Mater.* **2010**, *22*, 2685 – 2688.
[17] J. Cravillon, C. A. Schröder, R. Nayuk, J. Gummel, K. Huber, M. Wiebcke, *Angew. Chem. Int. Ed.* **2011**, *50*, 8067 – 8071; *Angew. Chem.* **2011**, *123*, 8217 – 8221.
[18] A. Carné-Sánchez, I. Imaz, M. Cano-Sarabia, D. Maspoch, *Nat. Chem.* **2013**, *5*, 203 – 211.
[19] M. Klimakow, P. Klobes, A. F. Thünemann, K. Rademann, F. Emmerling, *Chem. Mater.* **2010**, *22*, 5216 – 5221.
[20] C. Wiles, P. Watts, *Green Chem.* **2014**, *16*, 55 – 62.
[21] P. Poechlauer, J. Colberg, E. Fisher, M. Jansen, M. D. Johnson, S. G. Koenig, M. Lawler, T. Laporte, J. Manley, B. Martin, A. O'Kearney-McMullan, *Org. Process Res. Dev.* **2013**, *17*, 1472 – 1478.
[22] M. Rubio-Martinez, M. P. Batten, A. Polyzos, K.-C. Carey, J. I. Mardel, K.-S. Lim, M. R. Hill, *Sci. Rep.* **2014**, *4*, 5443.
[23] M. Rubio-Martinez, T. Leong, P. Juliano, T. D. Hadley, M. P. Batten, A. Polyzos, K.-S. Lim, M. R. Hill, *RSC Adv.* **2016**, *6*, 5523 – 5527.
[24] A. S. Munn, P. W. Dunne, S. V. Y. Tang, E. H. Lester, *Chem. Commun.* **2015**, *51*, 12811 – 12814.
[25] M. Gaab, N. Trukhan, S. Maurer, R. Gummaraju, U. Müller, *Microporous Mesoporous Mater.* **2012**, *157*, 131 – 136.
[26] K.-J. Wu, V. Nappo, S. Kuhn, *Ind. Eng. Chem. Res.* **2015**, *54*, 7554 – 7564.
[27] Y. Su, K. Kuijpers, V. Hessel, T. Noël, *React. Chem. Eng.* **2016**, *1*, 73 – 81.
[28] R. H. Perry, D. W. Green, *Perry's Chemical Engineers' Handbook*, McGraw-Hill, New York, **2008**.
[29] T. Noël, Y. Su, V. Hessel, *Top. Organomet. Chem.* **2015**, 1 – 41.
[30] G. Taylor, *Proc. R. Soc. London Ser. A* **1954**, *223*, 446 – 468.
[31] S. Heinz, D. Roekaerts, *Chem. Eng. Sci.* **2001**, *56*, 3197 – 3210.
[32] F. Jeremias, D. Fröhlich, C. Janiak, S. K. Henninger, *RSC Adv.* **2014**, *4*, 24073.
[33] S. K. Henninger, F. Jeremias, H. Kummer, C. Janiak, *Eur. J. Inorg. Chem.* **2012**, 2625 – 2634.

Received: December 23, 2015
Revised: February 22, 2016
Published online on April 14, 2016